ACS Chemical Neuroscience

Research Article

pubs.acs.org/chemneuro

Expedited Access to Vinaxanthone and Chemically Edited Derivatives Possessing Neuronal Regenerative Effects through Ynone Coupling Reactions

Matthew R. Chin,[†,‡] Katherine Zlotkowski,[†,‡] Michelle Han,[†] Saagar Patel,[†] Anders M. Eliasen,[†,‡] Abram Axelrod,[†] and Dionicio Siegel*[,†,‡]

[†]Department of Chemistry, The University of Texas at Austin, Austin, Texas 78712, United States

[‡]Skaggs School of Pharmacy and Pharmaceutical Sciences, University of California, San Diego, La Jolla, California 92039, United States

Supporting Information

ABSTRACT: The natural product vinaxanthone has demonstrated a remarkable capability to promote nerve growth following injury or transplantation. In rats following total transection of the spinal cord delivery of vinaxanthone enhanced axonal regeneration, remyelination and angiogenesis at the site of injury all leading to an improved reinstatement of motor function. Through the development of a new ynone coupling reaction, chemically edited derivatives of vinaxanthone have been prepared and studied for improved activity. The coupling reaction allows rapid access to new derivatives, wherein n ynone precursors provide n^2 vinaxanthone analogues. These compounds have been tested for their ability to promote neuronal regrowth using laser axotomy, severing axonal connections in *Caenorhabditis elegans*. This precise microsurgery using *C. elegans* allows a new in vivo approach for medicinal chemistry based optimization of neuronal growth promoting compounds.

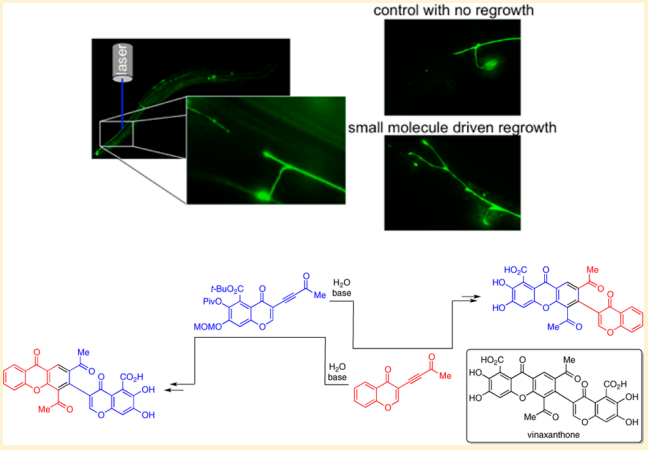

KEYWORDS: *Vinaxanthone, spinal cord injury, analogue synthesis, regeneration, laser axotomy, C. elegans*

There is a need for the development of small molecule-based therapeutics for the treatment of spinal cord injury, a condition currently lacking a cure. In the search for new leads for the treatment of spinal cord injury, the natural products vinaxanthone (**1**) and xanthofulvin (**2**) were discovered by extensive screening to identify compounds that prevent growth cone collapse (Figure 1). The natural products have since been found to possess remarkable regenerative effects in animal models of full spinal cord transection in combination with treadmill training[1] and alone[2] as well as to promote nerve growth following corneal transplant.[3] The compounds were coisolated from fungal extracts of *Penicillium* sp. SPF-3059 guided by an assay to identify inhibitors of semaphorin 3A (Sema3A)-mediated growth cone collapse.[4,5] Growth cone collapse by Sema3A occurs through modulation of the actin cytoskeleton and microtubules and results in failed regeneration of injured neurons.[6−8] Vinaxanthone and xanthofulvin prevent Sema3A-mediated growth cone collapse by disrupting Sema3A/plexin interactions.[9] Sustained administration of either natural product through continual infusion or the use of a solid matrix drug delivery system following complete spinal cord transection significantly increased the regeneration and survival of injured neurons, enhanced cellular survival, led to robust remyelination, and improved angiogenesis at the injury site, all leading to a notable recovery.[2] In addition, the combination of vinaxanthone treatment and treadmill training to encourage the correct rewiring led to restoration of hindlimb motor function.[1] Notably, there is no cytotoxicity observed at >1000 times the effective concentration, providing a good therapeutic window.[5] Interestingly, genetic removal of Sema3A function does not lead to the same regeneration following injury, suggesting that

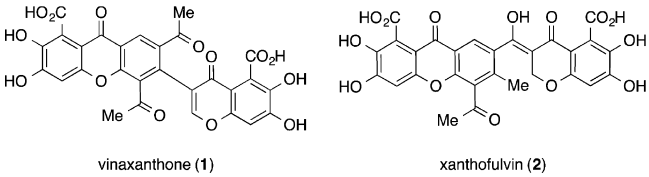

Figure 1. Structures of vinaxanthone (**1**) and xanthofulvin (**2**).

Received: October 3, 2014
Revised: January 22, 2015
Published: January 23, 2015

DOI: 10.1021/cn500237z
ACS Chem. Neurosci. 2015, 6, 542−550

Scheme 1. Key Dimerization Steps in Previous Syntheses of Vinaxanthone

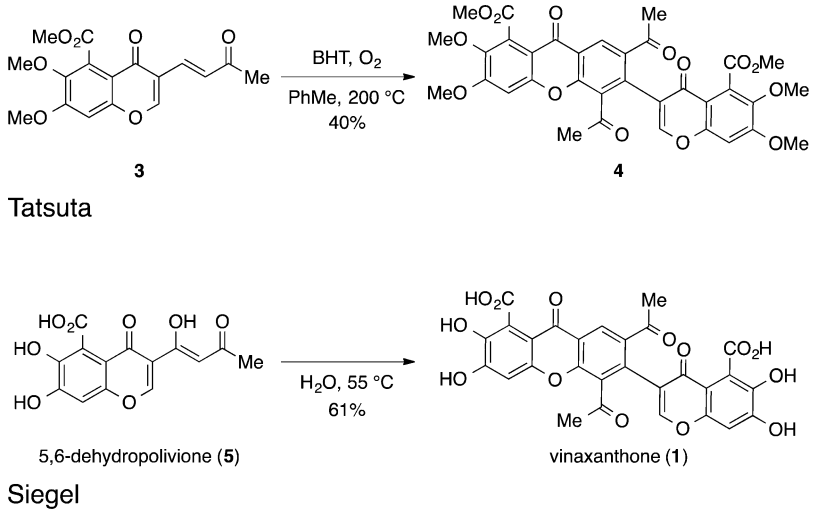

Scheme 2. Synthetic Strategy for Chemically Edited Vinaxanthone Analogues

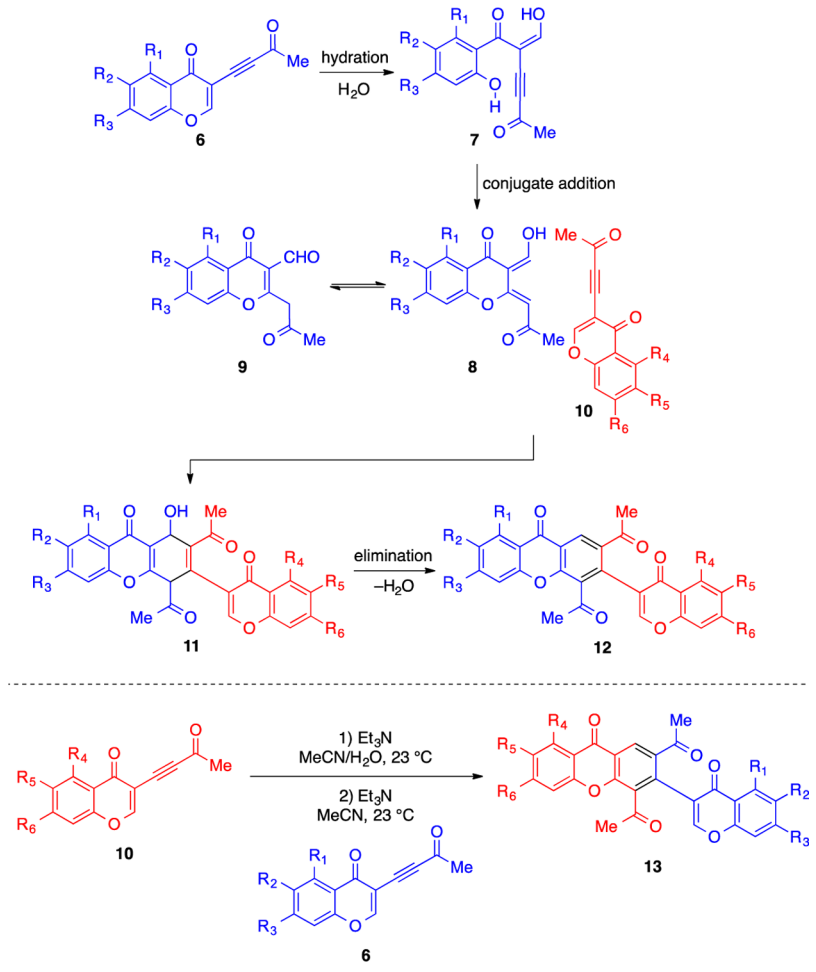

the inhibitory effects of the compounds against Sema3A are not solely responsible for the pronounced regeneration and that beneficial, off-target effects likely exist.[10] The potential polypharmacology of these compounds, blocking inhibition of regrowth and actively promoting regeneration, provides a pharmacological solution that has long been sought for treatment of spinal cord injury.[11] As a result of their remarkable regenerative effects, synthetic routes to both natural products have been developed and a common pathway for their formation in nature has been proposed.[12−14] Herein new chemistry is reported for the systematic preparation of analogues through novel ynone coupling reactions as well as an improved synthesis of vinaxanthone. Following the syntheses of the new, abridged analogues, the ability of the

DOI: 10.1021/cn500237z
ACS Chem. Neurosci. 2015, 6, 542−550

Scheme 3. Proof-of-Concept for the Ynone Coupling Reaction Generating Protected Vinaxanthone 16

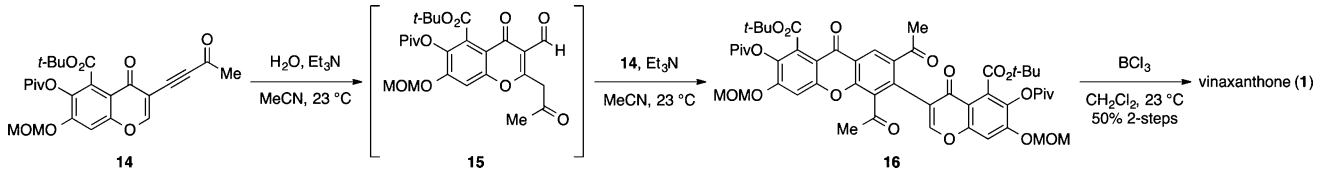

Scheme 4. Ynone Precursors and Coupling Reactions

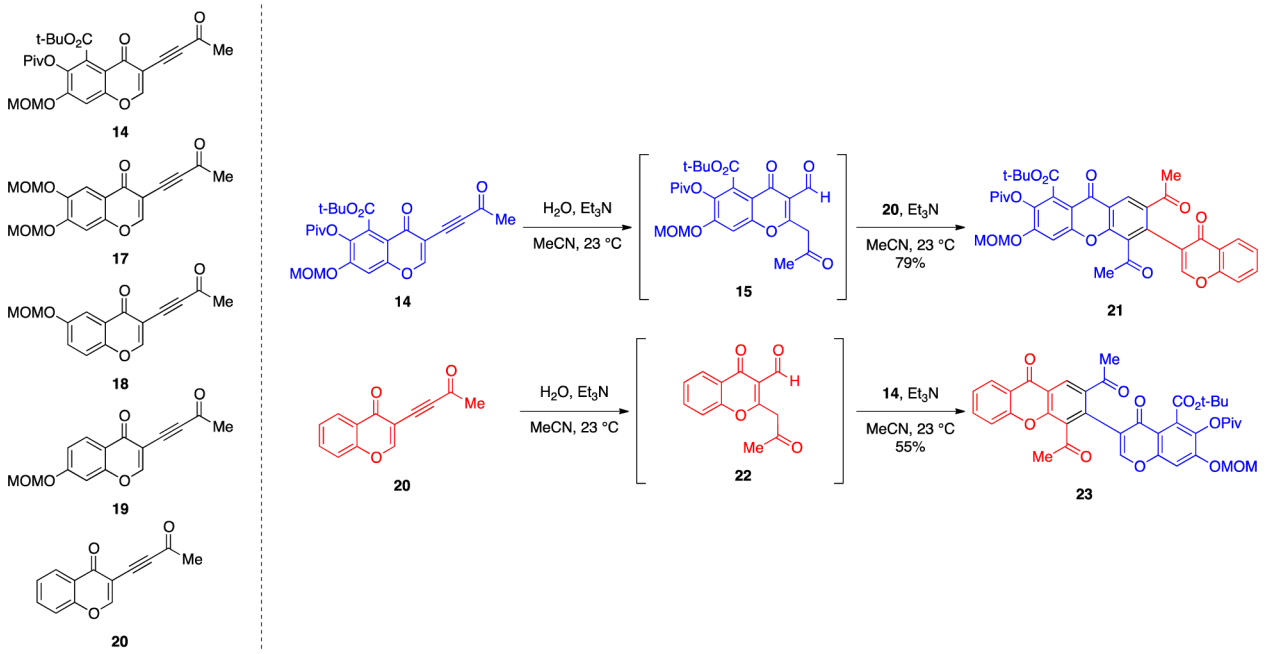

chemically edited derivatives to promote neuronal growth following injury was achieved using the nematode *Caenorhabditis elegans* and microsurgery with ultrafast laser axotomy.

Previous syntheses of vinaxanthone utilized the embedded symmetry of the molecule and employed dimerization reactions to generate the natural product from different monomeric precursors (Scheme 1). The first synthesis (of either molecule) by Tatsuta and co-workers utilized a Diels–Alder/oxidative aromatization sequence to combine two molecules of unsaturated ketone **3** at elevated temperature (200 °C) in the presence of air to generate permethylated vinaxanthone **4**.[12] More recently, our group utilized a biologically inspired dimerization of the putative natural product 5,6-dehydropolivione (**5**) to generate vinaxanthone (**1**).[14] Upon mild heating of a neutral, aqueous solution of the hypothetical C14 polyketide-based precursor 5,6-dehydropolivione (**5**), vinaxanthone was directly obtained in 61% yield. Following from this, we reported the first synthesis of xanthofulvin (**2**), removing ambiguity regarding an alternative structure for the same compound, 411J. However, given the greater inherent stability of vinaxanthone (xanthofulvin slowly decomposes in solutions when exposed to oxygen) and the similar biological profiles, we sought to develop a systematic method for the synthesis of vinaxanthone analogues to determine the structure activity relationship (SAR) as well as eventually optimize the biological performance.

However, if either of the reported synthetic approaches were to be used to generate analogues, these dimerization reactions would likely provide a statistical mixture of products, as the dimerizations lack electronically or sterically controlling elements that could differentiate the two fragments and select for their positioning, since the monomers either possess dual reactivity as a Michael donor/acceptor or, for Diels–Alder reactions, function as both a diene/dienophile. The lack of control limited the ability to efficiently produce edited derivatives with distinct xanthone (western region) and chromone (eastern region) cores. While one can access analogues through nonselective reactions a systematic method for analogue preparation is ideal, selectively providing a targeted compound and avoiding challenging chromatographic separations of isomers. In addition, the development of a new approach enables the syntheses of compounds based on the vinaxanthone core yet to be realized.

RESULTS AND DISCUSSION

To overcome the challenge of coupling two similar fragments while maintaining a convergent synthesis we sought to generate intermediates such as diene **8** which could be accessed from a parent ynone precursor **6** by hydration (Scheme 2). These dienes and/or the corresponding anions are predicted to undergo cycloaddition/dehydrative elimination reactions with parent ynones to generate the required xanthone cores.[15] Importantly, the electronics of the cycloaddition are in concert for the formation of the correct xanthone core. The relative positioning of the fragments by in situ reaction of one of the ynones prior to coupling has the added benefit of streamlining the syntheses of derivatives, whereby n ynones can generate n^2 analogues.

DOI: 10.1021/cn500237z
ACS Chem. Neurosci. 2015, 6, 542–550

Scheme 5. Vinaxanthone and Chemically Edited Derivatives[a]

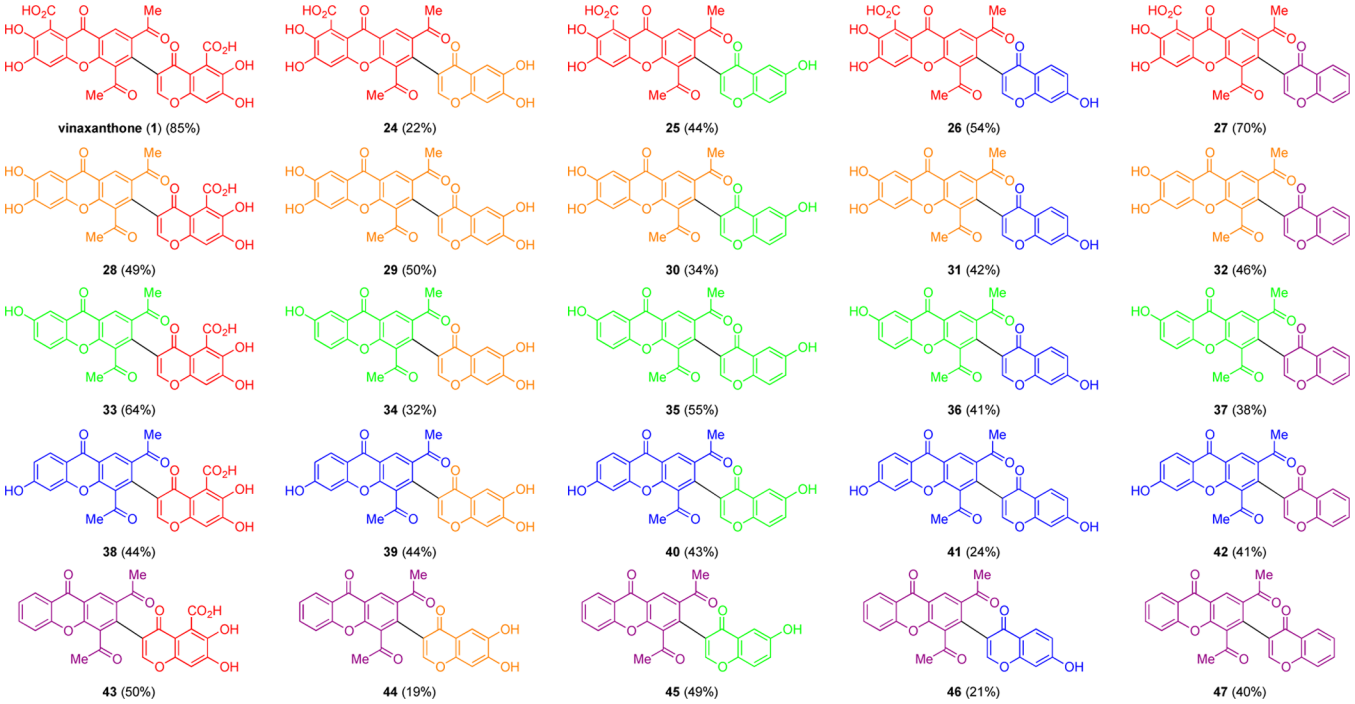

[a]Yields in parentheses over two steps: ynone coupling and deprotection.

Table 1. Optimization of Water-Mediated Dimerization of Ynone 14, Providing Protected Vinaxanthone 16

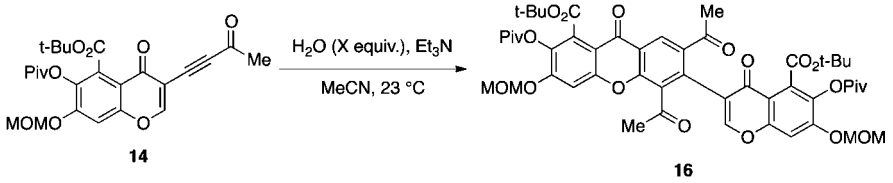

14 16

Entry	H_2O (equivalents)	% Yield
1	0	0%
2	0.1	65%
3	0.5	87%
4	1.0	67%
5	2.0	59%

To examine the hydration reaction generating an intermediate 3-formyl chromone shown for **15** (for the synthesis of vinaxanthone), ynone **14**[14] was treated with excess water and triethylamine at 23 °C (Scheme 3). This successfully transformed ynone **14** into the desired 3-formyl chromone **15** (in $CDCl_3$ **15** exists primarily in the aldehydic form) which was used directly. Gratifyingly, the addition of the rearranged product **15** to a solution of the starting ynone **14** and triethylamine in acetonitrile at 23 °C generated protected vinaxanthone **16**. Subsequent global deprotection of the six protecting groups was achieved with boron trichloride in methylene chloride to provide an alternative synthesis of vinaxanthone (**1**). This process has been further optimized to generate protected vinaxanthone **16** on the gram scale directly from ynone **14** using substoichiometric amounts of water (vida infra).

Five separate 3-ynone chromones were prepared in 4−9 steps from commercial starting material (Scheme 4; see the Supporting Information for syntheses). The ynone precursors were synthesized following a similar sequence that was utilized for the synthesis of ynone **14**. The five ynones were then combined systematically to generate vinaxanthone (**1**) and 24 analogues in protected form. As an example, the combination of ynone **14** with ynone **20** generated the protected vinaxanthone analogue **21** in 79% yield. Alternatively, subjecting ynone **20** to the water-mediated rearrangement followed by the addition of ynone **14** formed the protected isomeric vinaxanthone analogue **23** in 55% overall yield (Scheme 4). As a final step, cleavage of the protecting groups can be achieved using boron trichloride in methylene chloride at 23 °C or with dry HCl in methanol heated to reflux. The yields for the final products over two steps ranged from 19 to 85%. Applying this to all the precursors generated the 25 compounds in Scheme 5.

DOI: 10.1021/cn500237z
ACS Chem. Neurosci. 2015, 6, 542−550

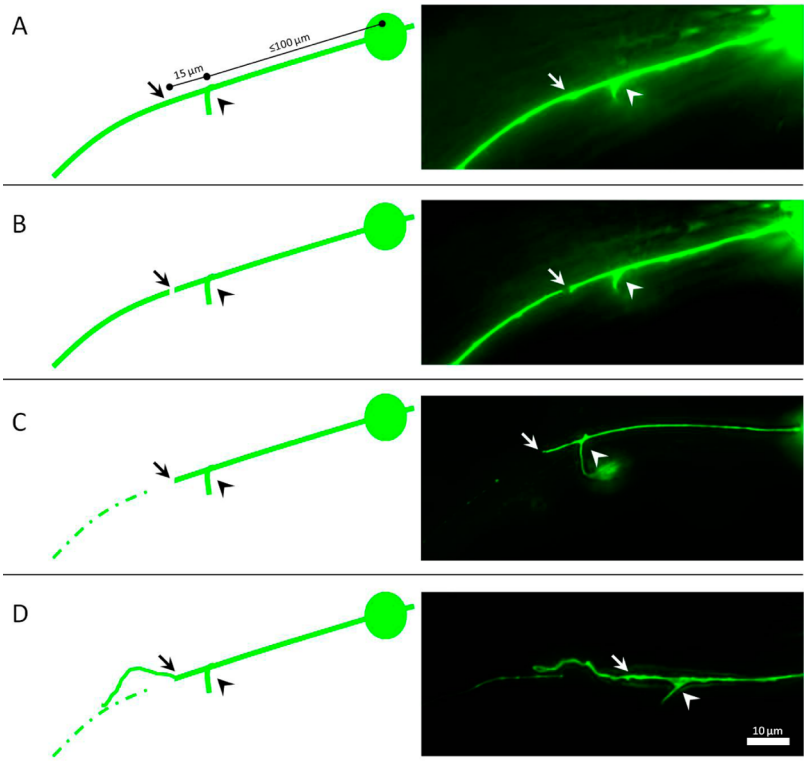

Figure 2. Representative images of in vivo laser axotomy. (A) Laser axotomy is performed on the PLM about 15 μm distal to the synaptic branch point when the branch is ≤100 μm from the cell body. (B) The injured neuron immediately following axotomy. (C) No regrowth from the severed proximal axon of control worms at 24 h postaxotomy. The distal fragment has begun to degenerate as seen by the faint, beaded appearance. (D) Regrowth of the severed proximal axon at 24 h postaxotomy. Arrows indicate the site of axotomy and arrowheads indicate the synaptic branch.

The water-mediated rearrangement and cycloaddition/elimination sequence was found to be quite efficient for dimerization when conducted with substoichiometric equivalents of water, instead of the initial discrete formation of 3-formyl chromone intermediates. This has provided the most convenient synthesis of vinaxanthone to date. Interestingly, the use of catalytic amounts of water (0.1 equiv) generated the vinaxanthone core in 65% yield. After optimization, 0.5 equiv of water generated protected vinaxanthone **16** in 87% yield (Table 1).

Laser Axotomy in *C. elegans*. *C. elegans* have several attributes that make them ideal for investigating regenerative responses coupled with medicinal chemistry in living organisms. Results from a single compound using the *C. elegans* axotomy model can be obtained in a matter of hours with the entire library being screened in a matter of days compared with murine models which require substantial amounts of time and resources. Importantly, the worm has proved pivotal in the discovery of numerous biological processes relevant to human health including apoptosis[16] and RNAi,[17−19] and has been developed as a model for the study of axon regeneration.[20] Its small size, well-characterized neurobiology, and transparency permit monitoring of neurons in living organisms via fluorescent labeling and therefore make the nematode particularly useful for chemical-neurobiological studies. Many genes that affect neuronal survival and axonal regeneration in vertebrate neurons have similar counterparts in *C. elegans*, further supporting its use as a biologically relevant model organism.[21] In addition, high throughput organism-based screens using *C. elegans* have proven to be useful for the identification of small molecules with phenotypic effects.[22,23] The use of *C. elegans* is presented herein for the first time as a tool for the optimization of the biological performance of compounds through medicinal chemistry.

Axonal injury can be induced in *C. elegans* by severing individual green fluorescent protein (GFP) labeled axons in live animals using highly precise laser microsurgery.[20] This surgery is then followed by monitoring for neuronal survival and growth. Laser axotomy in *C. elegans* has aided in the identification of a substantial number of genetic determinants of neuronal regeneration.[24−26] Although most of the axonal regeneration studies in *C. elegans* have primarily focused on the native promoters and suppressors of growth, the worm provides a unique platform for small molecule development. Along these lines high throughput screens have been developed to identify compounds from chemical libraries that can promote regeneration after laser axotomy.[27]

Laser axotomy was used to sever the posterior lateral microtubule (PLM) cells of *C. elegans*. These two mechanosensory neurons, which are responsible for the worm's reaction to light posterior touch, are located in the tail and extend longitudinally toward the midbody, one along the left and the other along the right side of the worm. Additionally, each of these forms a single synaptic branch with the ventral nerve cord.[28,29] The mechanosensory neurons have been used extensively in laser axotomy experiments and are ideal for examining regeneration due to their relatively large size and distinctive axonal morphology.[30] Furthermore, investigations involving neurodegeneration in human diseases have employed these neurons, establishing a relevant connection to the worm model.[31,32]

DOI: 10.1021/cn500237z
ACS Chem. Neurosci. 2015, 6, 542−550

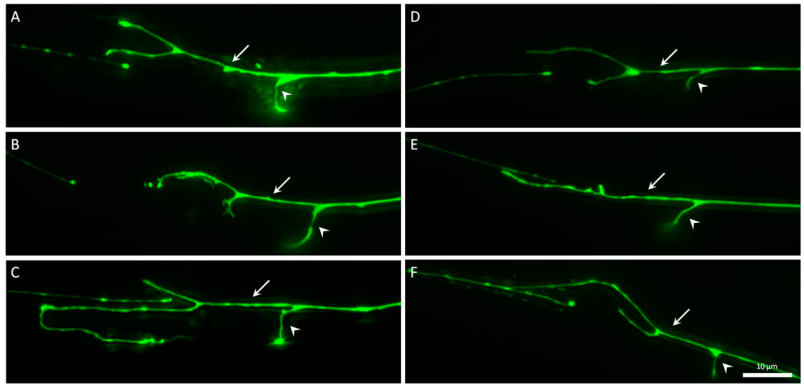

Figure 3. Regrowth of PLM neurons 24 h after laser axotomy. (A) Branching regrowth following treatment with 2 μM vinaxanthone. (B) Arching regrowth following treatment with 2 μM analogue **37**. (C) Regrowth with branching to the ventral nerve cord. (D) Branching regrowth following treatment with 2 μM analogue **37**. (E) Linear regrowth following treatment with 2 μM analogue **37**. (F) Regrowth with reconnection to the distal fragment. Arrows indicate the beginning of regrowth and arrowheads indicate the synaptic branch.

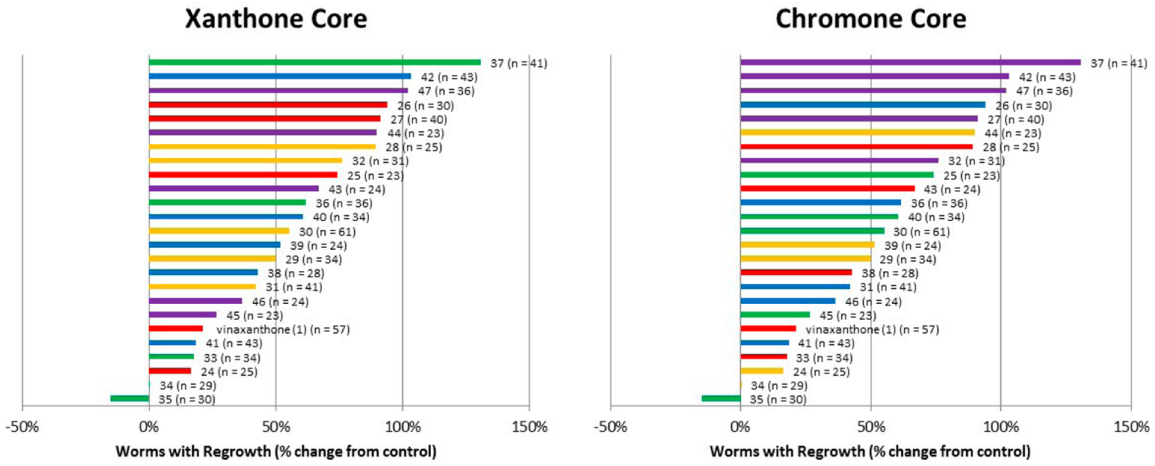

Figure 4. Worms exposed to vinaxanthone analogues exhibiting varying levels of neuronal regrowth, represented as a percent change relative to controls. Colors are provided for SAR comparisons.

Mechanosensory neurons severed beyond their synaptic branch provided a starting point for our microsurgeries as this branch has been implicated as a transition point in innate regenerative ability, where PLM neurons are able to regrow when severed proximal to their synaptic branch but not when severed distal to the branch point.[30] Severing the axon beyond the branch point, therefore, resulted in a standard with limited intrinsic regrowth following injury. Furthermore, this model utilizing an inhibitory branching environment might be particularly advantageous as many spinal cord neurons possess collateral branches that have been shown to influence regrowth potential.[33,34]

Small Molecule-Mediated Regeneration. Laser axotomy was used to sever the PLM of late L4-stage *C. elegans* (*zdIs5*) at a point approximately 15 μm distal to the synaptic branch point (Figure 2A). The distance of the synaptic branch point from the cell body in the nematodes was observed to vary slightly between worms. The greater the distance of injury from the cell body, the less likely regeneration will occur.[30] To standardize the location of axotomy and to maintain the potential for regrowth, nematodes possessing a synaptic branch with a maximum distance of 100 μm from the cell body to the branch point were selected as having the desired PLM morphology and were used in the experiments employing the analogues of vinaxanthone (**1**).

A characteristic series of events follows axotomy. The laser ruptures the neuron by creating a small break in the axon as a result of plasma formation and the generation of cavitation bubbles at the site of injury[35] (Figure 2B). Over the next few hours, the ends of the severed axon retract, increasing the gap between the fragments. The distal fragment begins to undergo degeneration, and lack of regrowth from the proximal axon results in a stump (Figure 2C). The distal fragment degeneration is characterized by the beading and disappearance of GFP and can be compared to Wallerian degeneration.[36] If the regeneration process is initiated, however, a growth cone forms on the proximal fragment and the axon will begin to extend as it regrows (Figure 2D). Occasionally, the regrowing axonal process finds its distal fragment; this fusion consequently prevents distal degeneration.[37]

When the axon was severed distal to the synaptic branch it was able to regrow in a small number of control worms (27%), and this potential for regrowth was enhanced by treatment with vinaxanthone (**1**). Based on these results, laser surgery was performed and nematodes were subsequently exposed to one of the vinaxanthone analogues. Regrowth of the severed proximal axon was quantified 24 h after axotomy by measuring from the beginning of new growth at the axonal injury site to the tip of the longest regrowing process. The process growths exhibited a variety of morphologies from virtually linear extension across

DOI: 10.1021/cn500237z
ACS Chem. Neurosci. 2015, 6, 542−550

the site of injury to arching around the axotomy scar as well as branching in search of their distal fragments, with some growths occasionally reaching the ventral cord in a manner similar to the synaptic branch (Figure 3). The regrowth usually occurred without connection to the distal fragment. Regrowth and reconnection to the distal portion was observed on occasion and was counted as positive for regrowth with its length measured to the point of reconnection. If growth was not observed from the proximal portion of the cut axon, it was regarded as negative for regrowth.

Worms treated with the analogues showed varying degrees of regeneration in both the number of worms exhibiting regrowth relative to controls and the lengths of the regrown neurons (see the Supporting Information). The analogue **37** (monohydroxylated xanthone core and bare chromone core) had the highest rate of regrowth, with a 130% increase from controls in the number of worms exhibiting regrowth morphologies (Figure 4).

Comparatively, vinaxanthone (**1**) showed a 21% increase in regrowth rate. Interestingly, analogue **34** had virtually no change in regrowth potential and analogue **35** had a 15% decrease in regrowth rate. In examining the data for structure–activity relationship (SAR) correlations, it was found that analogues **37**, **42**, **47**, **26**, and **27** specifically exhibited high levels of regrowth (over 90% increase). It is noteworthy that four of these five molecules possess the same abridged structures for their chromone cores. The dose–response relationships for vinaxanthone and the most potent analogue, **37**, were compared (Figure 5). Vinaxanthone exhibited a

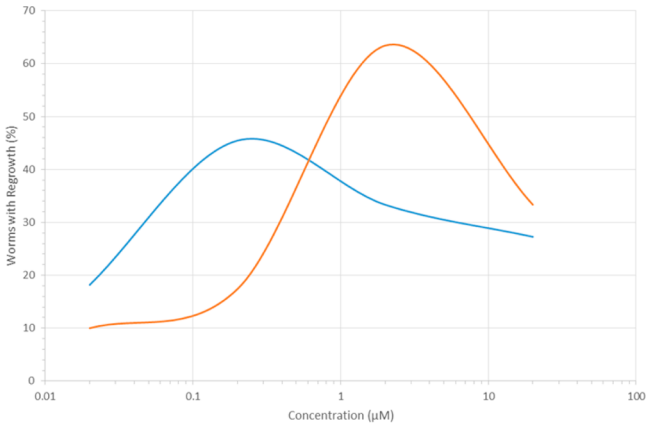

Figure 5. Dose–response relationship of worms exposed to vinaxanthone (blue line) and analogue **37** (orange line), showing a biphasic dose–response.

maximum biological activity at a lower concentration (0.2 μM), while analogue **37** was shown to induce an overall greater biological response albeit at higher concentration (2 μM). Interestingly, both compounds show decreased activity at 20 μM concentrations, demonstrating a biphasic dose–response.

CONCLUSIONS AND PERSPECTIVE

A new ynone coupling reaction has been developed, providing a rapid method for the exponential syntheses of chemically edited analogues of vinaxanthone (**1**). The sequence of hydration–cycloaddition–dehydration has also been applied to provide a second generation synthesis of vinaxanthone using catalytic water. Following from the syntheses of new derivatives, laser axotomy in *C. elegans* has effectively allowed the testing of the regrowth-inducing potentials of vinaxanthone and a library of chemically edited analogues. This has aided in the determination of the structure–activity relationship of the molecule as well as demonstrated that the functional group free chromone core is an important chromophore for in vivo regrowth. Using the ynone coupling reaction, additional analogues of vinaxanthone will be prepared and, following additional optimization using *C. elegans,* the compounds will be transitioned into additional organisms.

METHODS

Chemistry. *General Methods.* All reactions were performed in flame-dried round-bottom or modified Schlenk (Kjedahl shape) flasks fitted with rubber septa under a positive pressure of argon, unless otherwise indicated. Air-and moisture-sensitive liquids and solutions were transferred via syringe or canula. Organic solutions were concentrated by rotary evaporation at 20 Torr. Methylene chloride (CH_2Cl_2) and tetrahydrofuran (THF) were purified using a Pure-Solv MD-5 solvent purification system (Innovative Technology). Acetonitrile (MeCN) was purified using a Vac 103991 solvent purification system (Vacuum Atmospheres). Dimethoxyethane (DME) was purchased from Acros (99+%, stabilized with BHT), methanol (MeOH) was purchased from Sigma-Aldrich (99.8%, anhydrous), and ethanol (EtOH) was purchased from Pharmco-Aaper (200 proof, absolute). All other reagents were used directly from the supplier without further purification unless noted. Analytical thin-layer chromatography (TLC) was carried out using 0.2 mm commercial silica gel plates (silica gel 60, F254, EMD chemical) and visualized using a UV lamp and/or aqueous ceric ammonium molybdate (CAM) or aqueous potassium permanganate ($KMnO_4$) stain. Infrared spectra were recorded on a Nicolet 380 FTIR using neat thin film or KBr pellet technique. High-resolution mass spectra (HRMS) were recorded on a Karatos MS9 and are reported as m/z (relative intensity). Accurate masses are reported for the molecular ion $[M + Na]^+$, $[M + H]$, $[M^+]$, or $[M - H]$. Nuclear magnetic resonance spectra (^1H NMR and ^{13}C NMR) were recorded with a Varian Gemini instrument [(400 MHz, ^1H at 400 MHz, ^{13}C at 100 MHz), (500 MHz, ^{13}C at 125 MHz), (600 MHz, ^{13}C at 150 MHz)]. For $CDCl_3$ solutions, the chemical shifts are reported as parts per million (ppm) referenced to residual protium or carbon of the solvent; $CHCl_3$ δ H (7.26 ppm) and $CDCl_3$ δ D (77.0 ppm). For $(CD_3)_2SO$ solutions, the chemical shifts are reported as parts per million (ppm) referenced to residual protium or carbon of the solvents; $(CD_3)(CHD_2)SO$ δ H (2.50 ppm) or $(CD_3)_2SO$ δ C (39.5 ppm). Coupling constants are reported in Hertz (Hz). Data for ^1H NMR spectra are reported as follows: chemical shift (ppm, referenced to protium; s = singlet, d = doublet, t = triplet, q = quartet, dd = doublet of doublets, td = triplet of doublets, ddd = doublet of doublet of doublets, m = multiplet, coupling constant (Hz), and integration). Melting points were measured on a MEL-TEMP device without corrections.

General Procedure A for Ynone Dimerization. To a stirred solution of ynone (1.0 equiv) (intended xanthone side of protected vinaxanthone) and H_2O (1000 equiv) in MeCN (0.01 M) at 23 °C was added triethylamine (10 equiv). After 1 h, the reaction mixture was diluted with EtOAc, dried over Na_2SO_4, and concentrated in vacuo to give an amber oil. The crude aldehyde was diluted to 0.1 M with MeCN before the second ynone (1.0 equiv) (intended chromone side of protected vinaxanthone) and triethylamine (2 equiv) were added. The reaction mixture was stirred at 23 °C for 16 h. The reaction mixture was then concentrated to give crude protected vinaxanthone. The crude material was purified via silica gel column chromatography to give pure protected vinaxanthone analogue.

General Procedure B for Ynone Dimerization. To a stirred solution of ynone (1.0 equiv) in MeCN (0.1 M) at 23 °C was added a 1.0 M solution of H_2O in MeCN (0.5 equiv) and triethylamine (10 equiv). After 16 h, the reaction mixture was concentrated in vacuo to give crude protected vinaxanthone. The crude material was purified via

DOI: 10.1021/cn500237z
ACS Chem. Neurosci. 2015, 6, 542–550

silica gel column chromatography to give pure protected vinaxanthone analogue.

General Procedure A for Global Deprotection. To a stirred solution of protected vinaxanthone analogue (1.0 equiv) in CH_2Cl_2 at 0 °C was added a 1.0 M solution of boron trichloride in CH_2Cl_2 (2.0 equiv per protecting group). The reaction mixture was stirred at 23 °C for 1 h. The reaction mixture was then diluted with EtOAc and washed with brine (5×). The organic layer was dried over Na_2SO_4 and concentrated in vacuo to give crude vinaxanthone. Trituration with pentane/MeOH (ratio varies depending on substrate solubility) gave pure vinaxanthone analogue.

General Procedure B for Global Deprotection. A solution of protected vinaxanthone analogue (1.0 equiv) in 1.25 M methanolic HCl (10 equiv per protected group) was stirred at 65 °C for 8 h. The reaction was followed by aliquot ^{1}H NMR. The reaction mixture was then purged with N_2 and concentrated in vacuo to give crude vinaxanthone. Trituration with pentane/MeOH (ratio varies depending on substrate solubility) gave pure analogue vinaxanthone.

Nematode Cultures and Microscopy. *C. elegans* cultures were maintained on nematode growth medium (NGM) agar plates seeded with *Escherichia coli* OP50 bacteria at 22 °C according to established procedures.[38] The strain used for axotomy experiments was SK4005 (zdIs5 [mec-4::GFP + lin-15(+) (pSK1)]), which can be obtained from the Caenorhabditis Genetics Center. General maintenance of *C. elegans* was performed using an Olympus SZX16 stereomicroscope. GFP-labeled nematodes were visualized using an Olympus IX73 inverted microscope with a Prior Lumen 200 fluorescence illumination system. Laser axotomies were performed using the Olympus IX73 microscope (100×/1.40 NA objective) equipped with an Andor MicroPoint nitrogen pulsed dye laser (435 nm). Images were captured using a Hamamatsu Orca-flash2.8 digital camera and cellSens Dimension imaging software.

Small Molecule Treatment. Stock solutions of the small molecules were prepared in DMSO (12.5 mM) and subsequently diluted in M9 buffer to a final concentration of 0.04 mM (0.32% DMSO, v/v). Diluted solutions (200 μL) were spread over seeded NGM plates (35 × 10 mm, containing 4 mL of agar) and allowed to absorb to a final concentration of 2 μM. Nematodes were then transferred to these plates for small molecule treatment.

Laser Axotomy. Surgery was performed on late L4-stage *C. elegans* immobilized on 5% agarose pads and anesthetized with levamisole (3 μL, 1 mM in M9 buffer). Axons of the PLM were cut using a single laser pulse approximately 15 μm after the synaptic branch, but only when the branch point was ≤100 μm from the cell body. Only nematodes whose synaptic branch morphology met this requirement were used in the experiments. Nematodes were transferred to prepared NGM plates after the surgery, washed twice with M9 buffer (3 μL), and allowed to recover at 22 °C overnight. Axon regrowth was measured 24 h postaxotomy from the site of axotomy to the tip of the longest regrowing process ($n \geq 23$ worms). No growth from the proximal portion of the cut axon was recorded as zero regrowth. Growth of the synaptic branch was sometimes observed but was not included in regrowth measurements.

■ ASSOCIATED CONTENT

Supporting Information

Detailed experimental procedures, syntheses, and spectral characterization of compounds as well as laser axotomy and small molecule treatment experimentals. This material is available free of charge via the Internet at http://pubs.acs.org.

■ AUTHOR INFORMATION

Corresponding Author

*E-mail: drsiegel@ucsd.edu.

Funding

This work has been supported financially by the Welch Foundation (F-1694) and the NSF (CHE-1151708), which are gratefully acknowledged.

Notes

The authors declare no competing financial interest.

■ ACKNOWLEDGMENTS

We thank Mr. Sorey and Ms. Spangenberg for NMR assistance, Jon Pierce-Shimomura for helpful conversations regarding the use of *C. elegans*, and Adela Ben-Yakar for helpful conversations regarding laser axotomy.

■ REFERENCES

(1) Zhang, L., Kaneko, S., Kikuchi, K., Sano, A., Maeda, M., Kishino, A., Shibata, S., Mukaino, M., Toyama, Y., Liu, M., Kimura, T., Okano, H., and Nakamura, M. (2014) Rewiring of regenerated axons by combining treadmill training with semaphorin3A inhibition. *Mol. Brain 7*, 14.

(2) Kaneko, S., Iwanami, A., Nakamura, M., Kishino, A., Kikuchi, K., Shibata, S., Okano, H. J., Ikegami, T., Moriya, A., Konishi, O., Nakayama, C., Kumagai, K., Kimura, T., Sato, Y., Goshima, Y., Taniguchi, M., Ito, M., He, Z., Toyama, Y., and Okano, H. (2006) A selective Sema3A inhibitor enhances regenerative responses and functional recovery of the injured spinal cord. *Nat. Med. 12*, 1380−1389.

(3) Omoto, M., Yoshida, S., Miyashita, H., Kawakita, T., Yoshida, K., Kishino, A., Kimura, T., Shibata, S., Tsubota, K., Okano, H., and Shimmura, S. (2012) The semaphorin 3A inhibitor SM-345431 accelerates peripheral nerve regeneration and sensitivity in a murine corneal transplantation model. *PloS One 7*, e47716.

(4) Kumagai, K., Hosotani, N., Kikuchi, K., Kimura, T., and Saji, I. (2003) Xanthofulvin, a novel semaphorin inhibitor produced by a strain of Penicillium. *J. Antibiot. (Tokyo) 56*, 610−616.

(5) Kumagai, K., Ksihino, A., Hosotani, N., Ito, A., Saji, I., and Kimura, T. (2005) Nerve Regeneration in the Central Nervous System by a Semaphorin Inhibitor. *Sumitomo Kagaku*, 1−8.

(6) Pasterkamp, R. J., Giger, R. J., Ruitenberg, M. J., Holtmaat, A. J., De Wit, J., De Winter, F., and Verhaagen, J. (1999) Expression of the gene encoding the chemorepellent semaphorin III is induced in the fibroblast component of neural scar tissue formed following injuries of adult but not neonatal CNS. *Mol. Cell. Neurosci. 13*, 143−166.

(7) Pasterkamp, R. J., Anderson, P. N., and Verhaagen, J. (2001) Peripheral nerve injury fails to induce growth of lesioned ascending dorsal column axons into spinal cord scar tissue expressing the axon repellent Semaphorin3A. *Eur. J. Neurosci. 13*, 457−471.

(8) De Winter, F., Oudega, M., Lankhorst, A. J., Hamers, F. P., Blits, B., Ruitenberg, M. J., Pasterkamp, R. J., Gispen, W. H., and Verhaagen, J. (2002) Injury-induced class 3 semaphorin expression in the rat spinal cord. *Exp. Neurol. 175*, 61−75.

(9) Winberg, M. L., Noordermeer, J. N., Tamagnone, L., Comoglio, P. M., Spriggs, M. K., Tessier-Lavigne, M., and Goodman, C. S. (1998) Plexin A is a neuronal semaphorin receptor that controls axon guidance. *Cell 95*, 903−916.

(10) Lee, J. K., Chow, R., Xie, F., Chow, S. Y., Tolentino, K. E., and Zheng, B. (2010) Combined genetic attenuation of myelin and semaphorin-mediated growth inhibition is insufficient to promote serotonergic axon regeneration. *J. Neurosci. 30*, 10899−10904.

(11) Liu, K., Tedeschi, A., Park, K. K., and He, Z. (2011) Neuronal intrinsic mechanisms of axon regeneration. *Annu. Rev. Neurosci. 34*, 131−152.

(12) Tatsuta, K., Kasai, S., Amano, Y., Yamaguchi, T., Seki, M., and Hosokawa, S. (2007) The first total synthesis of vinaxanthone, a fungus metabolite possessing multiple bioactivities. *Chem. Lett. 36*, 10−11.

(13) Lösgen, S., Schlörke, O., Meindl, K., Herbst-Irmer, R., and Zeeck, A. (2007) Structure and biosynthesis of chaetocyclinones, new polyketides produced by an endosymbiotic fungus. *Eur. J. Org. Chem.*, 2191−2196.

(14) Axelrod, A., Eliasen, A. M., Chin, M. R., Zlotkowski, K., and Siegel, D. (2013) Syntheses of xanthofulvin and vinaxanthone, natural

DOI: 10.1021/cn500237z
ACS Chem. Neurosci. 2015, 6, 542−550

products enabling spinal cord regeneration. *Angew. Chem., Int. Ed. 52*, 3421−3424.
(15) Ghosh, C. K., Bhattacharyya, A., and Bandyopadhyay, C. (1984) Base-Catalyzed Deacylative Dimerization of 3-Acetylchromenone—A Facile Diels-Alder Reaction. *J. Chem. Soc., Chem. Commun.*, 1319−1320.
(16) Ellis, R. E., Yuan, J. Y., and Horvitz, H. R. (1991) Mechanisms and functions of cell death. *Annu. Rev. Cell Biol. 7*, 663−698.
(17) Tabara, H., Grishok, A., and Mello, C. C. (1998) RNAi in *C. elegans*: Soaking in the genome sequence. *Science 282*, 430−431.
(18) Tabara, H., Sarkissian, M., Kelly, W. G., Fleenor, J., Grishok, A., Timmons, L., Fire, A., and Mello, C. C. (1999) The rde-1 gene, RNA interference, and transposon silencing in *C. elegans*. *Cell 99*, 123−132.
(19) Fire, A., Xu, S. Q., Montgomery, M. K., Kostas, S. A., Driver, S. E., and Mello, C. C. (1998) Potent and specific genetic interference by double-stranded RNA in *Caenorhabditis elegans*. *Nature 391*, 806−811.
(20) Yanik, M. F., Cinar, H., Cinar, H. N., Chisholm, A. D., Jin, Y. S., and Ben-Yakar, A. (2004) Neurosurgery—Functional regeneration after laser axotomy. *Nature 432*, 822.
(21) El Bejjani, R., and Hammarlund, M. (2012) Neural Regeneration in *Caenorhabditis elegans*. *Annu. Rev. Genet. 46*, 499−513.
(22) Kwok, T. C. Y., Ricker, N., Fraser, R., Chan, A. W., Burns, A., Stanley, E. F., McCourt, P., Cutler, S. R., and Roy, P. J. (2006) A small-molecule screen in *C. elegans* yields a new calcium channel antagonist. *Nature 441*, 91−95.
(23) Burns, A. R., Kwok, T. C. Y., Howard, A., Houston, E., Johanson, K., Chan, A., Cutler, S. R., McCourt, P., and Roy, P. J. (2006) High-throughput screening of small molecules for bioactivity and target identification in *Caenorhabditis elegans*. *Nat. Protoc. 1*, 1906−1914.
(24) Gabel, C. V., Antonie, F., Chuang, C. F., Samuel, A. D. T., and Chang, C. (2008) Distinct cellular and molecular mechanisms mediate initial axon development and adult-stage axon regeneration in *C. elegans*. *Development 135*, 1129−1136.
(25) Hammarlund, M., Nix, P., Hauth, L., Jorgensen, E. M., and Bastiani, M. (2009) Axon Regeneration Requires a Conserved MAP Kinase Pathway. *Science 323*, 802−806.
(26) Ghosh-Roy, A., Wu, Z. L., Goncharov, A., Jin, Y. S., and Chisholm, A. D. (2010) Calcium and Cyclic AMP Promote Axonal Regeneration in *Caenorhabditis elegans* and Require DLK-1 Kinase. *J. Neurosci. 30*, 3175−3183.
(27) Samara, C., Rohde, C. B., Gilleland, C. L., Norton, S., Haggarty, S. J., and Yanik, M. F. (2010) Large-scale in vivo femtosecond laser neurosurgery screen reveals small-molecule enhancer of regeneration. *Proc. Natl. Acad. Sci. U. S. A. 107*, 18342−18347.
(28) Chalfie, M., and Sulston, J. (1981) Developmental genetics of the mechanosensory neurons of *Caenorhabditis elegans*. *Dev. Biol. 82*, 358−370.
(29) Chalfie, M., Sulston, J. E., White, J. G., Southgate, E., Thomson, J. N., and Brenner, S. (1985) The neural circuit for touch sensitivity in *Caenorhabditis elegans*. *J. Neurosci. 5*, 956−964.
(30) Wu, Z., Ghosh-Roy, A., Yanik, M. F., Zhang, A. Z., Jin, Y. S., and Chisholm, A. D. (2007) *Caenorhabditis elegans* neuronal regeneration is influenced by life stage, ephrin signaling, and synaptic branching. *Proc. Natl. Acad. Sci. U. S. A. 104*, 15132−15137.
(31) Goodman, M. B., and Schwarz, E. M. (2003) Transducing touch in *Caenorhabditis elegans*. *Annu. Rev. Physiol. 65*, 429−452.
(32) Syntichaki, P., and Tavernarakis, N. (2003) The biochemistry of neuronal necrosis: Rogue biology? *Nat. Rev. Neurosci. 4*, 672−684.
(33) Richardson, P. M., and Issa, V. M. K. (1984) Peripheral injury enhances central regeneration of primary sensory neurons. *Nature 309*, 791−793.
(34) Parikh, P., Hao, Y. H., Hosseinkhani, M., Patil, S. B., Huntley, G. W., Tessier-Lavigne, M., and Zou, H. Y. (2011) Regeneration of axons in injured spinal cord by activation of bone morphogenetic protein/Smad1 signaling pathway in adult neurons. *Proc. Natl. Acad. Sci. U. S. A. 108*, E99−E107.
(35) Rao, G. N., Kulkarni, S. S., Koushika, S. P., and Rau, K. R. (2008) In vivo nanosecond laser axotomy: cavitation dynamics and vesicle transport. *Opt. Express 16*, 9884−9894.
(36) Chen, L. Z., and Chisholm, A. D. (2011) Axon regeneration mechanisms: Insights from *C. elegans*. *Trends Cell Biol. 21*, 577−584.
(37) Neumann, B., Nguyen, K. C. Q., Hall, D. H., Ben-Yakar, A., and Hilliard, M. A. (2011) Axonal Regeneration Proceeds Through Specific Axonal Fusion in Transected *C. elegans* Neurons. *Dev. Dyn. 240*, 1365−1372.
(38) Brenner, S. (1974) Genetics of *Caenorhabditis elegans*. *Genetics 77*, 71−94.

DOI: 10.1021/cn500237z
ACS Chem. Neurosci. 2015, 6, 542−550